Large Solid Rocket Motor safety analyses:

Thermal effects issues

Dr F.Chassagne
Missile safety expert
DGA/DT/CAEPE
33167 Saint Médard en Jalles, France

S. Bordachar
Explosive safety advisor, DGA/INSP/IPE
5 bis avenue de la Porte de Sèvres
75509 Paris Cedex 15

Abstract

Our ability to manage the explosive risks associated with Large Solid Rocket Motors when manufactured, transported, handled and stored is obviously crucial as some of these situations can involve several tons of solid propellants.
A mishap reference scenario, focused on HD 1.3 effects, has been defined by the explosive safety authorities leading to residual ambient propellant fire expansion as a result of a LSRM large pieces fragmentation.
Modelling this type of scenario still poses a great challenge in terms of scientific knowledge and safety assessment. In that way, some experimental and theoretical works were carried out in the last few years to investigate solid propellant combustion mechanisms at ambient conditions and radiative transfer properties associated with. Precisely, large Eddy Simulation Techniques were studied with the hypothesis that large eddies drive the overall fire flow structure and the hydrodynamics properties. For combustion, the number of length scales that control physical and chemical phenomena is problematic and acceptable compromises must be found in order to develop a model that correctly predict the heat transfer of such a fire.

Introduction

General principles of explosive safety risk management in France

If we consider the accident academic model constituted with the hazard source (industrial site…), hazard flux (propagation, toxic species dispersion, fire and explosion) and targets submitted to damage (personnel, material), the explosive risk management process can be articulated into three general principles:

1. source risk reduction,
2. accident effects limitation (action on the propagation vector),
3. accident consequences limitation (action on exposed sites)

Two regulations co exist in France: one relative to health and safety at work (rules and directives regarding the workers exposition to explosive risks, the other dealing with the potential consequences of an explosive site mishap on the surroundings and environment. The subsequent studies analyze the “fire phenomenon” and assess its consequences through modeling and focus precisely on:

Report Documentation Page

Form Approved
OMB No. 0704-0188

1. REPORT DATE	2. REPORT TYPE	3. DATES COVERED
JUL 2010	**N/A**	**-**

4. TITLE AND SUBTITLE
Large Solid Rocket Motor safety analyses: Thermal effects issues

5a. CONTRACT NUMBER
5b. GRANT NUMBER
5c. PROGRAM ELEMENT NUMBER

6. AUTHOR(S)

5d. PROJECT NUMBER
5e. TASK NUMBER
5f. WORK UNIT NUMBER

7. PERFORMING ORGANIZATION NAME(S) AND ADDRESS(ES)
DGA/DT/CAEPE 33167 Saint Médard en Jalles, France

8. PERFORMING ORGANIZATION REPORT NUMBER

9. SPONSORING/MONITORING AGENCY NAME(S) AND ADDRESS(ES)

10. SPONSOR/MONITOR'S ACRONYM(S)
11. SPONSOR/MONITOR'S REPORT NUMBER(S)

12. DISTRIBUTION/AVAILABILITY STATEMENT
Approved for public release, distribution unlimited

13. SUPPLEMENTARY NOTES
See also ADM002313. Department of Defense Explosives Safety Board Seminar (34th) held in Portland, Oregon on 13-15 July 2010, The original document contains color images.

14. ABSTRACT
Our ability to manage the explosive risks associated with Large Solid Rocket Motors when manufactured, transported, handled and stored is obviously crucial as some of these situations can involve several tons of solid propellants. A mishap reference scenario, focused on HD 1.3 effects, has been defined by the explosive safety authorities leading to residual ambient propellant fire expansion as a result of a LSRM large pieces fragmentation. Modelling this type of scenario still poses a great challenge in terms of scientific knowledge and safety assessment. In that way, some experimental and theoretical works were carried out in the last few years to investigate solid propellant combustion mechanisms at ambient conditions and radiative transfer properties associated with. Precisely, large Eddy Simulation Techniques were studied with the hypothesis that large eddies drive the overall fire flow structure and the hydrodynamics properties. For combustion, the number of length scales that control physical and chemical phenomena is problematic and acceptable compromises must be found in order to develop a model that correctly predict the heat transfer of such a fire.

15. SUBJECT TERMS

16. SECURITY CLASSIFICATION OF:			17. LIMITATION OF ABSTRACT	18. NUMBER OF PAGES	19a. NAME OF RESPONSIBLE PERSON
a. REPORT	b. ABSTRACT	c. THIS PAGE			
unclassified	**unclassified**	**unclassified**	**SAR**	**38**	

- heat release rate and its effects on the personnel (burns,…), potential structural weakness of buildings parts,
- smoke flow trajectory whose composition varies a lot in function of chemical species involved in the combustion mechanisms (intoxication source for personnel, fire propagation vector too)
- extinction waters which can lead to pollution and contamination

Large Solid Rocket Motor and propellants safety issues

Our ability to manage the explosive risks associated with Large Solid Rocket Motors when manufactured, transported, handled and stored is obviously crucial as some of these situations can involve several tons of solid propellants.
We focus here only on HTPB/AP composite propellants with rather large critical diameter, currently classified in France as 1.3 hazard division. This classification and specifically the non detonable ability is mainly based on small scale tests like Large Scale Gap test and Super Large Scale Gap test (with a 20 Kbars threshold), good friability and combustion under high pressure results to address the main mechanisms leading to detonation.

The possibility, no matter how improbable it is, of an explosive event for such a large system cannot obviously be ignored. Propellants of Hazard Division 1.3 are characterized by the fact that, unless heavily confined, their reaction does not result in the generation of high blast pressures, energy being released over a period measured in seconds or longer.
To give management an estimate of the risks, one must begin with an analysis of the situations in which these large systems are being used or might be used, the hazards which might be expected in these life cycle phases, and the possible results: In 2004, Both Explosive and Nuclear safety authorities expressed some concerns regarding the lack of data involved with large solid rocket motor explosion and fire consequences and the too conservative methods used in safety studies associated with assembly, check out and storage phases.
The interest has been raised within MoD to take advantage of the recent advances in the field of civilian fire safety engineering and some funding was allocated to MoD/DGA/CAEPE for conducting some experiments and modelling in association with universities like the Laboratory of Combustion and Détonics (CNRS) in Poitiers.
The objective of the experimental part of this project was to refine the existing data by doing different types of test in atmospheric conditions: some were intended to determine the infrared signature of AP/HTPB/Al flame plume by radiative heat flux measurements, IR thermal imaging and IR spectrometry. This was performed for two propellant compositions in order to highlight the main role played by Al/Al2O3 particles on thermal radiation to the surroundings at 1 atm. Within other test setup, in situ temperature and emissivity measurements were made at several standoff distances so as to obtain points of measure at least in different zones. Moreover these data were not only determined at the near-infrared narrow bandwidth but also at the mid-infrared narrow bandwidths λ =4.5μm and λ =4.66μm in order to provide new data on the radiative emission properties of such a flame.
For project modeling issues, both reference scenario and simulation strategies were defined to assess the ability of computational fluid dynamics and field models to fulfil MoD requirements.

1. Ambient propellant fire phenomenology

For this particular scenario associated with for instance a large rocket motor fragmentation through its structural weaknesses, the potential hazard is mainly due to thermal radiation and the direct impingement of the resulting fire. The development and the behaviour of the flame as well as the decisive parameters (dimensions, temperature, and duration) are generally

varying and strongly affected by the environment (e.g. wind, buildings architecture, vegetation etc).

Twenty five years ago a complete study on aluminized solid propellant fire under atmospheric conditions was carried out and concluded that such a flame plume could be schematically shared into three cones as shown in Figure 1 [1].
The primary cone just above the burning surface is where gaseous reactions between AP and HTPB decomposition products take place, with a flame temperature rising up to 2500K. AP/HTPB/Al solid propellant combustion is globally controlled by chemical kinetics at 1atm. Oxidizer and fuel decomposition products react into a premixed flame, or into a primary diffusion flame including finite kinetics [2, 3, 4]. Furthermore aluminum droplets are ignited and start burning into this zone which is very slightly affected by air cooling through the sides. Initial aluminum solid particles merge at TMelt = 933°K on the propellant burning surface and most of them burn very close to the propellant surface, yielding Aluminum oxide (Al2O3), whose size does not exceed 1-2 µm [5]. Left aluminum particles (unburnt Al) can form liquid aggregates on the propellant surface and are dragged up to the gaseous mixture. Their size can vary from 10 µm to 300 µm and mainly depends on the coalescence process. That is why the size distribution of aluminum droplets is a critical parameter which is still not so well-known at one atm, mainly due to the extremely strong flame environment (high temperature and optically thick media).

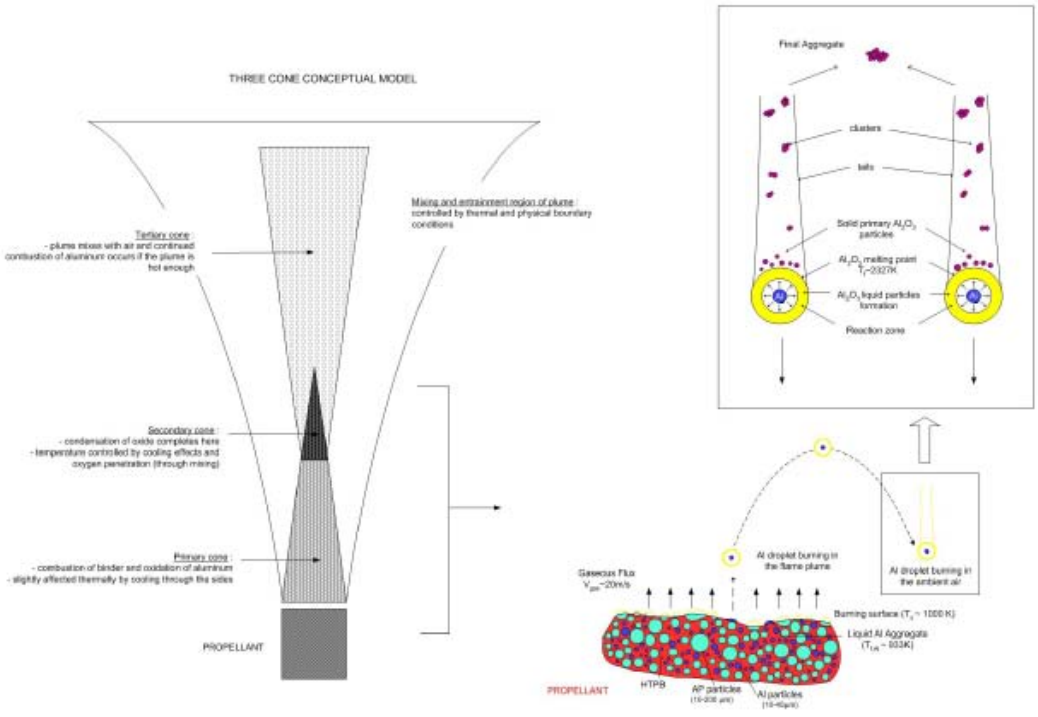

Figure n° 1: Propellant fire conceptual model and scheme of aluminum droplet combustion into the propellant gas mixture [1, 6]

The secondary cone is characterized by the completion of aluminum droplet combustion and the condensation of aluminum oxide. Plume temperature curves until 2350°K (just above the melting point of pure alumina) due to the cooling effects and oxygen penetration through the mixing. More precisely, aluminum droplets burn in the vapor phase because of the lower boiling point compared with the final combustion product Al2O3.

The reaction is believed to be limited by the diffusion of oxidizer towards the droplet and the outward of gaseous aluminum. The flame zone at 1 atm is located in the region r/r0=3-6 [7], where r and r0 are the radial coordinate and droplet radius, respectively. Homogeneous reaction takes place in the droplet flame zone between the gaseous aluminum and the oxidizer (oxygen in ambient atmosphere or carbon dioxide and water vapor in propellant gas mixture).
The oxidized products consist of gaseous sub oxides such as AlO, AlO2, Al2O, Al2O2 and condense in the flame zone to form Al2O3 smoke. The condensation proceeds via heterogeneous chemical reactions at the surface of alumina particles and the resulting particles are liquid and spherical in the reaction zone while final aggregates are solid in the air mixing zone. Al2O3 particle growth is then characterized by simultaneous coagulation and coalescence [6].
The tertiary cone and the mixing region are indeed the places where aluminum oxide final aggregates are formed and dispersed around. Temperature rapidly falls down due to mixing with ambient air.
Ten years later this whole conceptual model was refined by ”in situ” temperature and emissivity measurements using pyrometric and spectrometric methods at various locations above the burning surface [9]. It was showed that solid propellant operating with high Aluminum rate acts roughly as a gray body in the 600-1200 nm wavelength range and some measures of flame spectral emissivity were made in the near-infrared narrow bandwidth.
However flame characteristics (high temperature levels, high heterogeneity due to droplet combustion) make the experimental measurements extremely difficult and dramatically increase measurement uncertainties.
Moreover the previous works did not clearly point out the key role the Al/Al2O3 particles play on the thermal radiation to the surroundings, as it was made within a rocket motor exhaust plume [9]. The elaboration of efficient methods to depict the thermal environment of such a flame plume still remains and more accurate experimental data are needed to develop numerical tools that could predict the thermal impact of AP/HTPB/Al propellant fires at atmospheric pressure. It also implies to use current experimental techniques which have been developed for the last decades and to adapt them to such large scale tests.

2. Large ambient propellant fire modeling requirements

Preliminary: Field model in fire safety

As long as detailed spatial distributions of physical properties are not required, and the two layer description reasonably approximates reality, zone models are quite reliable. However, by their very nature, there is no way to systematically improve them. The rapid growth of computing power and the corresponding maturing of computational fluid dynamics (CFD), has led to the development of CFD based “field” models applied to fire research problems.
The application of “Large Eddy Simulation” (LES) techniques to fire is aimed at extracting greater temporal and spatial fidelity from simulations of fire performed on the more finely meshed grids allowed by ever faster computers.
The phrase LES refers to the description of turbulent mixing of combustion products with the local atmosphere surrounding the fire, this process still being extremely difficult to predict accurately.
“The basic idea behind the LES technique is that the eddies that account for most of the mixing are large enough to be calculated with reasonable accuracy from the equations of fluid dynamics. The hope (which must ultimately be justified by comparison to experiments) is that small-scale eddy motion can either be crudely accounted for or ignored” – Howard Baum, NIST Fellow emeritus

Validation issues and MoD requirements

The crucial point for fire modeling assessment is the ability to measure the difference between one model predictions and experimental data or between two model predictions or experimental databases. The standard ASTM E 135: Standard Guide for Evaluating the Predictive Capability of Deterministic Fire Models is of great interest.

The following techniques have to be used simultaneously:

- Comparing model results with explicit physics formula: This validation method can be done locally but is limited to simple formulations where an analytical solution can emerge.
- Comparing several models results on the same reference case: It some coherence on results appears, we can have some hope that the real solution is not far from these results. Confidence in the simulation is increased but experimental validation still needed.
- Directly comparing model results with experimental data: In this case, the uncertainty associated with the experimental results plays an important role, equivalent to that of calculated data.

MoD/ DGA requirements for modeling: Project CNRS/LCD and DGA CAEPE

Criteria	*Requirement*	*Flexibility*
Specification on input data	Experimental tests on SME HTPB/AP propellant s are to be privileged Literature results are to be used cautiously	Negotiable
Specification on hydrodynamic model	Navier Stockes equations and solid conduction equations must be solved in conditions representative of a fire: this part defines the director schemes to properly simulate a fire and gives some details on the way input data, combustion model, particulates radiative and turbulence models, numerical methods, output data, validation criteria should be presented.	No negotiable Turbulence resolution method to be chosen by university.
Specification on combustion model	A pyrolysis model and a heat generation source term shall be introduced in the model	No negotiable
Specification on radiative heat transfer model	The model must take into account all the radiative exchanges : particles (alumina, Al,…) and gaseous combustion products .If a T4 formulation is used, the model must discriminate between radiative heating inside the flame and outside the flame. A local formulation inside the flame and based on calorific debit ratio is possible	No negotiable Negotiable
Specification on combustion products and particulates	The transport equation can be solved using a species generation term proportional to the combustion rate. Each specie to have its own transport equation.	Negotiable
Specification on boundary conditions	The boundaries conditions must be versatile	No negotiable
Specification on output data	The output data must incorporate both global and local thermal fluxes characteristics , temperature, hydrodynamic data All the information on the present species in the gaseous mesh is to be available	No negotiable
Validation criteria on output results	Validation criteria must be defined	No negotiable
Specification on reports	The reports must enable validation, alter expertise and new simulation studies	Negotiable
Software specification	Open source, Fire Dynamic Simulator from BFRL/NIST privileged	Negotiable

3. Experimental investigations

3.1 Medium scale tests – phase1 [2005-2008]

All the experimental tests operate with AP/HTPB/Al-based 20 cm side cubic item (lateral inhibition) and two propellant compositions (20% and 4% of Aluminium in mass) are tested within this first setup. The solid propellants are produced by the SME Company (SNPE Group) and are typically used for defence or spatial applications. They are both ignited by some reacting pyrotechnic powder homogeneously laid on the propellant surface.

	%PA	%PBHT	%Al	d_{PA}	Dimensions (H*L*l)
Butalane	68	12	20	200μm - 90μm - 10μm	24cm*21cm*18cm
Butalite	82	14	4	400μm - 200μm - 10μm	24cm*21cm*18cm

This ignition system was validated by preliminary tests and is used during the whole present study. Besides, as the lateral surfaces are inhibited by a polymer-based protection, the solid propellant cube burns along one dimension as a cigarette.

Large View Tests:
Radiative heat flux is measured by eight Medtherm transducers located at 1-2 m distance from the propellant cube and at 1-2 m height from the initial propellant surface (Fig.2). All the captors are equipped with a sapphire window to avoid measuring diffusive heat flux. During the test, heat flux transducers are water-cooled and their supports are covered by a thermal protection. Furthermore flame radiance intensity is determined using two AGA782 infrared cameras held at 10 m aside the propellant sample. The first (AGA782 SWB) and the second one (AGA782 LWB) are respectively composed of one near IR band filter [3-5.5 µm] (with 97.5% transmittance) and one far IR band filter [7-11.5 µm] (with 97.5% transmittance). Their temperature measurement ranges from 300°C to 1500°C with an accuracy of ±0.4% and the atmospheric transmission coefficient is assumed to be nearly equal to 1. The emission spectrum of the plume is additionally assessed with a HGH-SPR314 spectrometer working between 3 µm and 14 µm and whose spectral resolution is 1.5%. The infrared cameras and spectrometer are calibrated against a large PYROX source whose diameter is 110 mm and emissivity is 0.99.

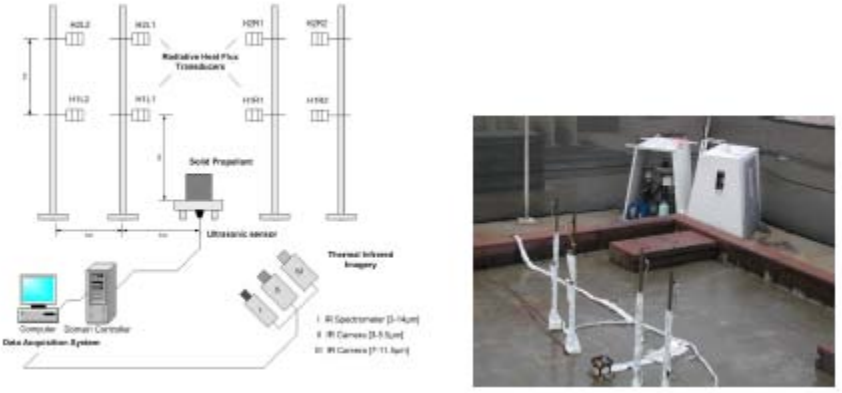

Figure n° 2 : Scheme of the Large View Test Setup

On the other hand, solid propellant burning rate is measured by a US Panametrics ultrasound sensor, stuck at the bottom of the sample (Fig.3). The measurement is local, instantaneous and based on the propagation of an acoustic wave into the burning propellant. The ultrasonic signal is emitted by the captor at a frequency of 500 Hz, reflected at the air-propellant interface and received by the same sensor. Data are collected at 500 Hz during the first 40 seconds, and then at 1 Hz until the end of the test.

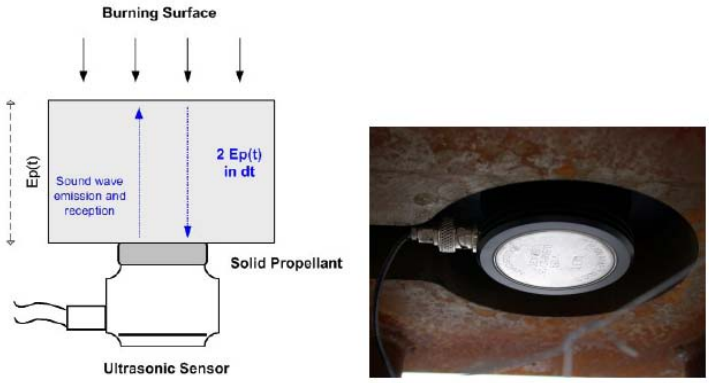

Figure n° 3: Schematic view and picture of the ultrasound system

Tests within graphite chimney

In situ flame temperature and local spectral emissivity are measured by pyrometers at three standoff distances above the initial propellant surface (Z1 = 6 cm, Z2 = 26 cm and Z3 = 46 cm) (Fig. 4). A 47.5 cm diameter graphite chimney and graphite sight tubes are devised to support all the captors and to resist to high temperatures. Notice that all the sight tubes are hollow tubes with one end at an angle to avoid the agglomeration of alumina solid particles inside. A nitrogen purge system is also implemented so as to eject smokes from the tubes.

This setup is based on validated experimental techniques and consists in pointing two pyrometers on the same space volume [9]. An IMPAC two-colour pyrometer with narrow bandwidths at 0.90 µm and at 1.05 µm is used to infer the plume temperature. As aluminised solid propellant acts as a graybody between 600 nm and 1200 nm [8], the local true flame temperature can then be accessed from the ratio of the intensities measured at each wavelength.

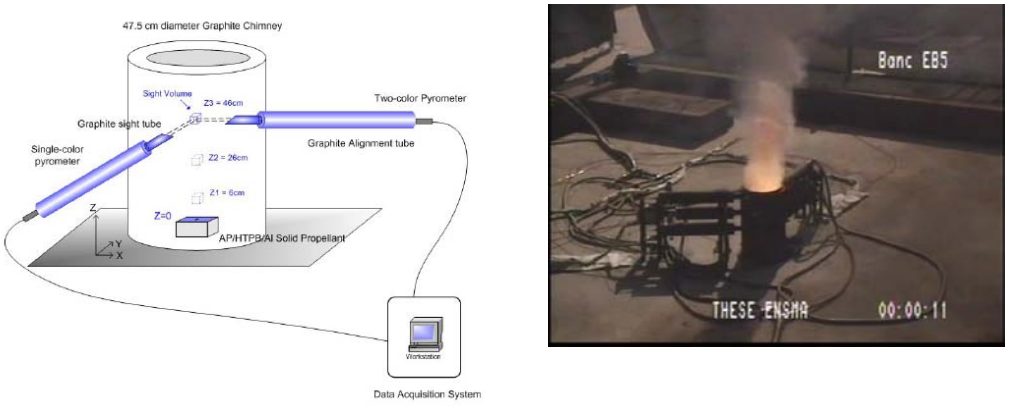

Figure n° 4: Principle of local temperature and spectral emissivity measurement

Then, pointing the single and the two-colour pyrometers on the same sight volume and assuming that the test is repeatable, flame spectral emissivity is deduced from the following relation at three narrow bandwidths (0.9 μm, 4.50 μm and 4.66 μm):

$$\epsilon(\lambda, T) = \exp\left[\frac{C_2}{\lambda}\left(\frac{1}{T} - \frac{1}{T_\lambda}\right)\right] \qquad (2)$$

$\epsilon(\lambda,T)$: spectral emissivity of the flame at wavelength λ and for the flame temperature T
T : Flame Temperature measured by the two-colour pyrometer

A two-colour IMPAC ISQ 5-LO pyrometer is used to measure the flame true temperature with narrow bandwidths located at λ =0.90μm and λ =1.05μm. The same pyrometer IMPAC ISQ 5-LO is also implemented to infer the radiance temperature at L =0.90μm. The accuracy of this apparatus is ±0.3%. Radiance temperatures at 4.50μm and 4.66μm are measured by two single colour Heitronics KT19II pyrometers whose accuracy is ±[0.5_C + 0.7%(Tbox-Tsource)]. All the pyrometers are calibrated against a large PYROX source to operate between 300°C and 2500°C.

Figure n° 5: Sight and alignment tubes

Notice that such a method is not relevant to the 4% Al-composed propellant which does not act a priori as a graybody source. That is why the extraction of in situ temperature and spectral emissivity has just been studied with the 20% Al composition.

Influence of the original Al-ratio on the propellant burning rate
The solid propellant burning rates are compared for the two compositions. In both cases quasi steady state is nearly achieved at 50 s after ignition, a time considered as the end of the ignition system effects. The time-averaged burning rate is 1.42 mm/s ±0.02 mm/s operating with the 20% Aluminised propellant and it is 1.10 mm/s ±0.04 mm/s with the 4% Aluminium one. In other words, higher aluminium rate in mass is, faster the solid propellant burns.
Heat release rate from Al droplet combustion contributes to increase the flame temperature and also the heat flux back to the propellant surface which controls the burning rate. This result is in good agreement with the computed adiabatic flame temperature which is pretty much higher for the 20% Al composition (Tf (20%Al) = 3182 °K) than for the 4% Al one (Tf (4%Al) = 2731 °K).
Furthermore, as solid propellant flame strongly depends on pressure, the measured values are weaker than AP/HTPB/Al burning rates achieved in solid propellant rocket motor combustion chamber at higher pressures (1 mm/s here vs 1-10 cm/s at 10-100 atm) .

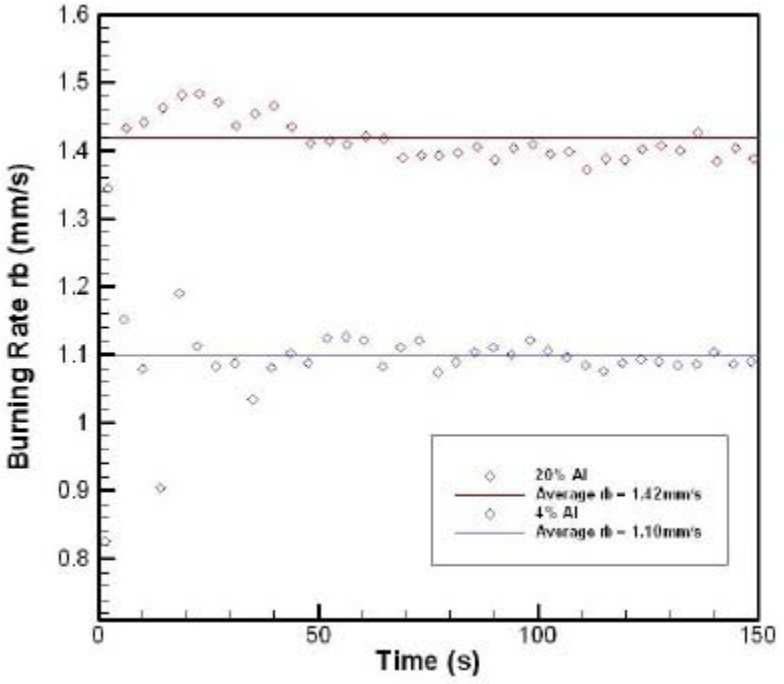

Figure n° 6: Propellant thickness and burning rate time evolution

AP / HTPB / 4% Al

Left Side	Average Radiative Heat Flux (kW/m^2)	Right Side
H1L1	6.2	8.2	H1R1
H2L1	2.8	2.9	H2R1
H1L2	2.1	2.5	H1R2
H2L2	1.4	1.6	H2R2

AP / HTPB / 20% Al

Left Side	Average Radiative Heat Flux (kW/m^2)	Right Side
H1L1	19.2	17.8	H1R1
H2L1	8.2	7.6	H2R1
H1L2	6.0	7.2	H1R2
H2L2	4.1	4.3	H2R2

Table n° 1: Radiative heat flux measurements aside and above the burning propellant

Influence of original Al-ratio on flame radiation to the surroundings

Radiative heat transfer to the surroundings is pretty much improved with the increasing Al-ratio as reported in Table 1. Average radiative heat flux is almost three times greater when operating with the 20% Al propellant than with the 4% Al one whatever the captor location. The influence of the initial aluminium ratio is observed even at 2 m distance, so quite far away from the propellant surface. At 1 m height from the reacting source, flame radiation is mainly induced by burning aluminium droplets.

Temperature into this plume area is very high, as shown in the further part, and Al droplet combustion is going on. On the contrary, most of the Al droplet combustion is completed at 2 m height so that flame plume is mainly composed of alumina particles and agglomerates. Plume temperature falls down due to the mixing with the ambient air and that explains the curving of the heat flux at 2 m height.

Finally, although differences between left and right side heat flux levels are not so large, AP/HTPB/Al flame plume cannot be considered as thermally symmetric mainly because of the aluminium agglomeration process that does not induce a symmetric spatial droplet distribution in the gas phase.
On the other hand, the infrared views display the internal structure of the plume for the two aluminised propellant compositions in two bandwidths where Al/Al2O3 droplets are particularly emissive (Fig n° 7.).
The unit is the radiance temperature of the flame contour, calculated from the measured intensity. Referencing to the conceptual model previously described, three main areas can be observed in both cases:
- The hottest zone just above the burning propellant surface where gas reactions take place and where Al droplets start burning
- The secondary cone where aluminium combustion and condensation of oxide complete
- The tertiary cone where flame plume mixes with air and where Al droplet combustion can occur if the plume is hot enough.
In the [3-5.5 µm] narrow bandwidth, radiance temperature is nearly 150°C higher for the 20% Al composition than for the 4% Al one whatever the location into the flame plume. This difference is even larger between 7 µm and 11.5 µm mostly because of Al/Al2O3 droplet and Al2O3 particle radiation properties in the far IR region.
As shown in the following part, Al2O3 solid particles are mainly emissive in the far infrared region so that the highest radiance temperatures are achieved in the [7-11.5 µm] bandwidth for the 20% Al composition. On the contrary the highest radiance temperatures are achieved for the 4% Al composition in the [3-5.5 µm] bandwidth, i.e. where the main gas emission bands (CO, CO2, H2O and HCl bands) are located. In this case flame radiation seems to be mostly induced by gas mixture and particularly by species such as CO and CO2 whose emission bands are the most significant respectively at 4.65 µm and 4.25 µm, as reported by spectrometric measurements (Fig. below).

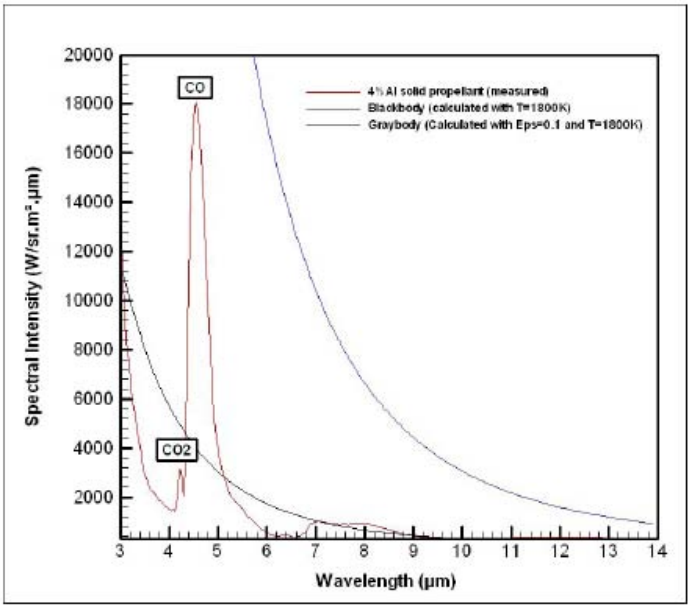

Figure n° 6: Spectrometric measurements (4%Al, 1atm):

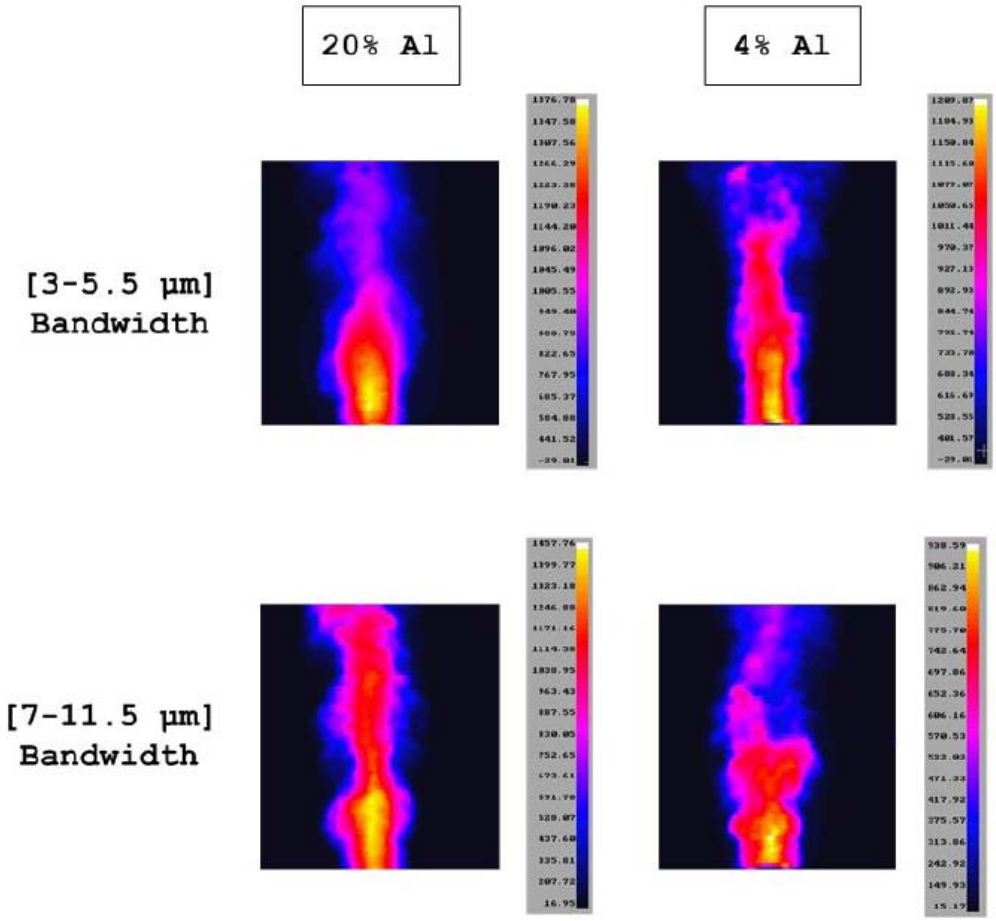

Figure n° 7: Infrared plume signature for two AP/HTPB/Al compositions (4% Al and 20% Al) at 1atm (t=30s)

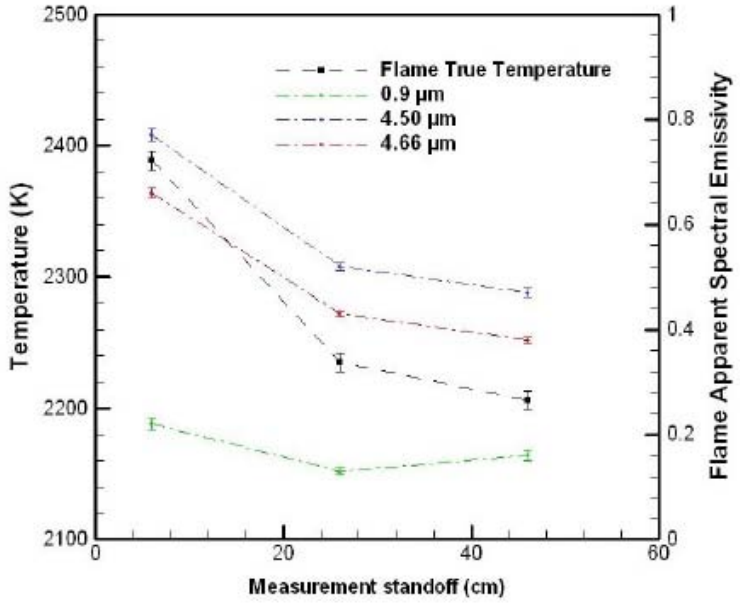

Figure n° 8: Temperature and flame spectral emissivity measurements (20%Al, 1atm)

Now let us deal with in situ measurements which enable to collect some data on the local flame true temperature and local spectral emissivity of AP/HTPB/20%Al solid propellant
Two different zones can be observed:

• The first one corresponds to the primary cone, which is close to the burning propellant surface (at 6 cm standoff distance) and where the flame true temperature (Tf = 2389 ±7 °K) is greater than alumina melting temperature (Tf = 2327 ±7 °K). As this area is highly loaded in burning Al droplets, it is very emissive from the mid infrared region. Indeed flame spectral emissivity rises up to 0.77 ±0.011 and 0.66 ±0.009 respectively at 4.50 μm and 4.66 μm while it is only 0.22 ±0.011 at 0.9 μm.

• The second one represents the secondary cone in which aluminium droplet combustion and aluminium oxide condensation complete. Flame true temperature drops to 2235 ±7 °K and 2206 ±7 °K respectively at 26 cm and 46 cm standoff distances. In the same way, spectral emissivities fall down in this region due to the temperature decrease and also to the changing flame composition. Indeed both flame true temperatures at 26 cm and 46 cm are less than alumina melting temperature.

Solid alumina particles may occur in this zone where condensation of aluminium oxides and Al droplet combustion are being completed. So flame emissivity that is much weaker at 0.9 μm than in the mid-infrared region may be mostly involved by alumina solid particles in this plume area. Although the flame plume is very heterogeneous and such in situ measurements are difficult to be set, these local values represents the thermal characteristics of the aluminized propellant flame and remain close to those reported by Diaz et al. who conducted spectrometric and pyrometric measurements within a more confined graphite chimney. Furthermore the key role Al2O3 particles play on the flame radiation has been pointed out once again and is now reinforced by comparison of flame spectral emissivity with the alumina particle one in the infrared region (Fig n° 9.).

Experimental data of Al2O3 emission properties were collected by Sarou Kanian et al. [12] for three alumina solid particle temperatures (T _ TAl2O3 melting) at the [1.8-9 μm] narrow bandwidth and are directly compared with the AP/HTPB/20%Al flame emission data. As it was expected, the radiative emission of aluminized propellant flame seems to be controlled by Al2O3 particle radiation.

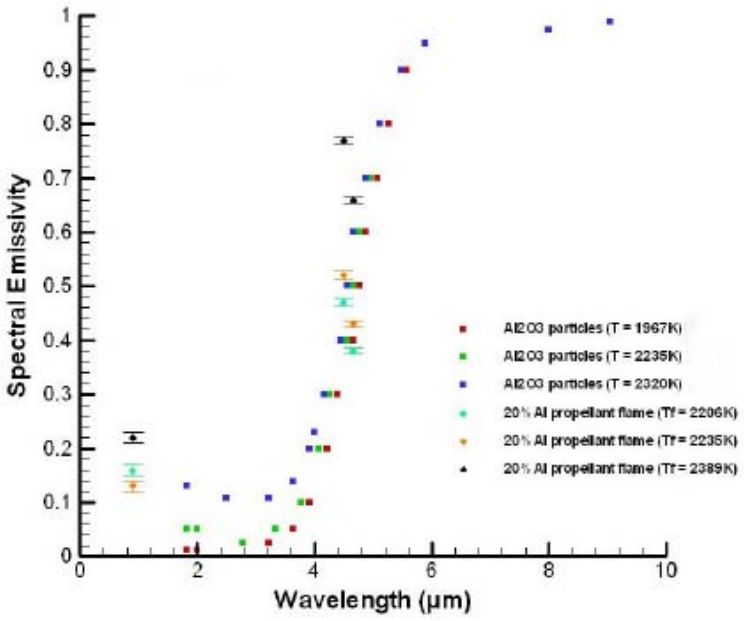

Figure n° 9: Comparison of the propellant flame spectral emissivity with the Al2O3 particles one [12] in the IR region

Flame spectral emissivity follows up the alumina solid particle one so that it is pretty greater in the mid IR than at around 1 μm. While aluminized propellant flame is considered as a graybody source from 600 nm to 1200 nm [8], a similar simplification cannot be assumed in the mid infrared. That makes even more complex the future modelling of aluminized solid propellant fire, specially the modelling of radiative heat transfer to the surroundings.
Finally let us notice the gaseous absorption role of carbon monoxide CO at 4.50 μm that could explain the greater spectral emissivity values obtained at this narrow bandwidth than at 4.66 μm.

Conclusion on phase1 tests

The three-cone conceptual model of aluminized solid propellant fire is pointed out by non intrusive diagnostic methods such as pyrometry, spectrometry and thermal imagery and testing two different AP/HTPB/Al propellant compositions. It is refined by adding new experimental data in the primary and secondary zones, which show how the role of burning Al droplets and aluminium oxide particles is significant on flame radiation to the surroundings and toward the burning propellant surface. This is confirmed by the comparison of the flame spectral emissivity with the alumina solid particle one making in situ measurements both in the near- and mid- infrared. It is revealed that AP/HTPB/20%Al flame emission follows up Al2O3 particles emission and that AP/HTPB/20%Al flame cannot be considered as a graybody source in the mid-infrared. Furthermore the role of gas radiation is limited to very concentrated gas species such as CO or CO2 and still remains less important than the particle one.

3.2 Experimental results (scaling effects) – phase2 [2009-2011]

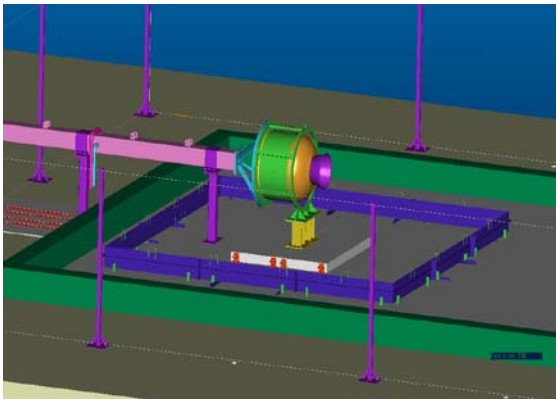

A third stage of a ballistic missile (2 tons of propellant) tested on fuel fire: thermal effects measurement

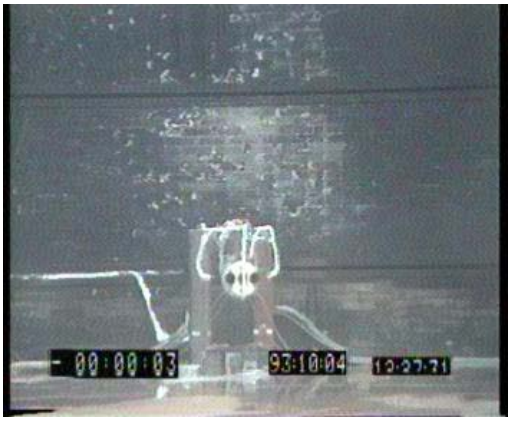

1 m square propellant fire on fully instrumented 160 mm inert mock up

Figure n°10 and 11: Large scale test (classified)

4. Modeling issues

The FDS software developed by the Building Fire Research Institute of NIST (USA) is the core of the modeling strategy in the way it should be possible to take advantage of all the validated assumptions and optimizations built for traditional fuel fire but common to ambient propellant fire: low mach numbers fluid dynamics, droplets Lagrangian tracking method, heat transfer calculation….

FDS Hydrodynamic model

Thanks to the increasing memory storage capacity it becomes possible to numerically predict physical phenomena as complex as they are. However the main difficulty to simulate propellant fire is the number of length scales that control physical and chemical phenomena. For instance the height of the propellant flame is on the order of hundred microns while the large eddy length scale is around 1m. For this reason physically acceptable compromises must be found in order to develop a model that correctly predicts the heat transfer of such a fire. Based on the CFD simulator named FDS the model described below has been adapted to propellant combustion.

An approximate form of the Navier-Stokes equations appropriate for low Mach number applications is used in the model. The approximation involves the filtering out of acoustic waves while allowing for large variations in temperature and density. The computation is treated as a Large Eddy Simulation (LES) in which the sub-grid scale dissipative processes are modelled. Following the analysis of Smagorinsky [7] the viscosity can be modelled as:

$$\mu_{LES} = \rho\left(C_s\Delta\right)^2\left(2\overline{\overline{D}}:\overline{\overline{D}} - \frac{2}{3}(\nabla \mathrm{u})^2\right)^{\frac{1}{2}}$$

where C_s is an empirical constant, Δ is a length on the order of the size of a grid cell and the deformation term is related to the dissipation function.

FDS Radiative heat transfer modelling

The radiative transport equation (RTE) for an absorbing/emitting and scattering medium is computed by a Finite Volume Method that divides the radiation spectrum into a few wavelength bands .

$$\mathrm{s}\cdot\nabla I_\lambda(\mathrm{x},\mathrm{s}) = -\left[\kappa(\mathrm{x},\lambda)+\sigma_s(\mathrm{x},\lambda)\right]I(\mathrm{x},\mathrm{s}) + \kappa(\mathrm{x},\lambda)I_b(\mathrm{x},\lambda) + \frac{\sigma_s(\mathrm{x},\lambda)}{4\pi}\int_{4\pi}\Phi(s,s')I_\lambda(\mathrm{x},\mathrm{s}')d\Omega'$$

Where $I_\lambda(\mathbf{x},\mathbf{s})$ is the radiation intensity at wavelength λ, $\mathbf{s}$ is the direction vector of the intensity, $\kappa(\mathbf{x},\lambda)$ and $\sigma_s(\mathbf{x},\lambda)$ are the local absorption and scattering coefficients, respectively, and $I_b(\mathbf{x})$ is the emission source term. In comparison of the droplets scattering that is prominent the gas scattering can be neglected in our case and the RTE becomes

$$\mathrm{s}\cdot\nabla I_n(\mathrm{x},\mathrm{s}) = \kappa_n(\mathrm{x},\lambda)\left[I_{b,n}(\mathrm{x},\lambda) - I(\mathrm{x},\mathrm{s})\right],\ \mathrm{n}=1\ldots\mathrm{N}$$

Where I_n is the intensity integrated over the band n, and κ_n is the appropriate mean absorption coefficient inside the band.

On the other hand the radiation-droplet interaction must be solved for both the accurate prediction of the radiation field and for the droplet energy balance. Therefore the gas phase absorption and emission (e.g. eq.()) is temporarily neglected for simplicity and the computed RTE is written as :

$$\mathbf{s}\cdot\nabla I_{\lambda}(\mathbf{x},\mathbf{s}) = -[\kappa_d(\mathbf{x},\lambda)+\sigma_d(\mathbf{x},\lambda)]I(\mathbf{x},\mathbf{s}) + \kappa_d(\mathbf{x},\lambda)I_{b,d}(\mathbf{x},\lambda) + \frac{\sigma_d(\mathbf{x},\lambda)}{4\pi}\int_{4\pi}\Phi(s,s')I_{\lambda}(\mathbf{x},\mathbf{s}')d\Omega'$$

where κ_d is the droplet absorption coefficient, σ_d is the droplet scattering coefficient and $I_{b,d}$ is the emission term of the droplets. $\Phi(s,s')$ is a scattering phase function that gives the scattered intensity from direction s' to s. The local absorption and scattering coefficients are calculated from the local number density N(x) and mean diameter $d_m(x)$ as

$$\kappa_d(x,\lambda) = N(x)\int_0^{\infty} f(r,d_m(x))C_a(r,\lambda)dr$$

$$\sigma_d(x,\lambda) = N(x)\int_0^{\infty} f(r,d_m(x))C_s(r,\lambda)dr$$

where r is the droplet radius and C_a and C_s are absorption and scattering cross sections, respectively, given by Mie theory.

4.1 Modeling strategy

This chapter briefly presents the modeling strategy defined to tackle thermal issues associated with ambient propellant fires.
First, a 1D thermal heat transfer model is used to predict the initiation delay of an aluminized propellant solid block, then due to volume consideration a propellant flame boundary condition representative of AP/HTPB solid propellant combustion in thermo chemical equilibrium conditions is defined at the solid surface .

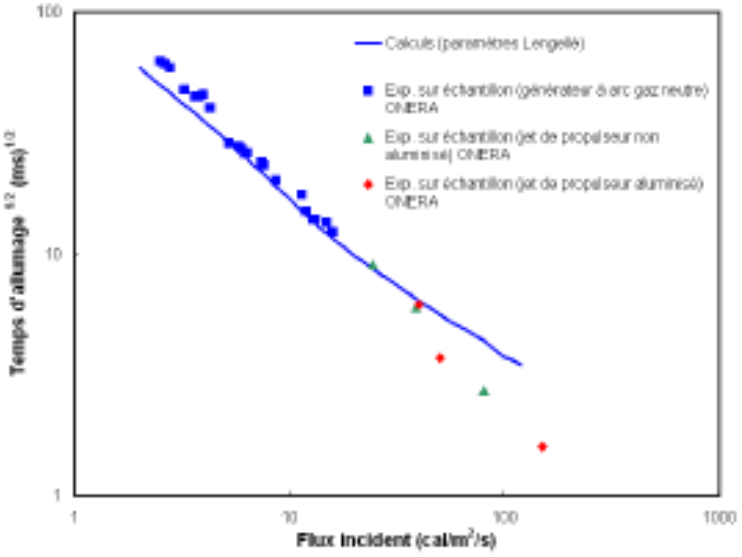

Figure n° 12: Initiation delay vs incident flux

	Butalane	Butalite
$T_f^{ad}(K)$	3087	2732
Y_{H_2}	2,2%	1,2%
Y_{CO}	23,2%	21,3%
Y_{HCl}	14,8%	22,7%
Y_{H_2O}	6,3%	22,6%
$Y_{Al_2O_3}$(L)	33,9%	7,4%
Y_{N_2}	8,1%	9,7%
Y_{CO_2}	1,6%	10,9%
Y_{O_2}	0,04%	0,2%

(b)	Butalane	Butalite
ρ_p (kg/m^3)	1807	1701
%Al en masse	18	4
v_c^{exp} (mm/s)	1,41	1,09
V_g (m/s)	23,2	16,6
$\dot{m}_g''$ (kg/m^2/s)	2,31	1,78
S_{pyro} (m^2)	0,0378	0,0378
$\dot{m}_{Al,l}$ (kg/s)	1,75E-02	2,80E-03

Figure n° 13: Propellant flame boundary condition (thermo chemical equilibrium, 1 atm)

The solid propellant surface temperature is equal to the adiabatic flame temperature calculated in atmospheric conditions. The burnt gases flow rate is directly derived from the experimental propellant regression rate.

The condensed phase composed of liquid Aluminum droplets is addressed by a gas-particle Eulerian-Lagrangian model defined in order to compute Al droplets' trajectory into the burnt gases. The force term **f** represents the momentum transferred from the Al droplets to the gas.

$$f = \frac{1}{2}\frac{\sum \rho C_D \pi r_d^2 \left(u_d - u\right)\left|u_d - u\right|}{\delta x \delta y \delta z}$$

where C_D is the drag coefficient, r_d is the droplet radius, u_d is the velocity of the droplet, u and ρ are respectively the velocity and the density of the gas, and δxδyδz is the volume of the grid cell. The trajectory of an individual droplet is governed by the equation:

$$\frac{d}{dt}\left(m_d u_d\right) = m_d g - \frac{1}{2}\rho C_D \pi r_d^2 \left(u_d - u\right)\left|u_d - u\right|$$

where m_d is the mass of the droplet and the drag coefficient C_D is a function of the local Reynolds number.

The initial droplet size distribution is expressed in terms of its Cumulative Volume Fraction (CVF), a function that relates the fraction of the Aluminium volume (mass) transported by droplets less than a given diameter. The mass and energy transfer is modelled by the following semi-empirical Al droplet combustion law adapted from []:

$$\begin{cases} \dfrac{dm_{Al}}{dt} = -\rho_{Al}\dfrac{\pi}{2}\dfrac{k}{n} d_{Al}^{3-n} \\ m_{Al} c_{p,Al}\dfrac{dT_d}{dt} = S_d h_d \left(T_g - T_d\right) - \dfrac{dm_{Al}}{dt} \times hv \end{cases}$$

where
$$n = 1{,}8$$
$$k = 85\left(X_{O_2} + X_{H_2O} + 0{,}7 X_{CO_2} - 1{,}5 X_{HCl}\right)^{0,9} p^{0,4}\ ,$$

X_i means the species molar fraction, p is the burnt gas pressure., m_{Al}, ρ_{Al}, d_{Al} and S_{Al} are respectively the mass, density, diameter and surface area of the Al droplet. h_d is the heat transfer coefficient which depends on Re, r_d, Pr and the thermal conductivity k. T_d and T_g are the droplet and the burnt gas temperatures while h_v is the Aluminium heat of vaporisation.

In atmospheric conditions the Al droplets oxidation plays a major role so a mixture fraction model is implemented for this part of the combustion process.

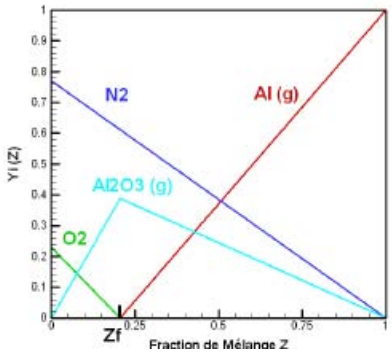

Figure n° 14: Mixture fraction model for gaseous phase

Radiative properties of Al droplets and AL2O3 are determined through Mie theory and the Dombrowsky model is used to take into account both their spectral and thermal dependencies. The temperature chosen for the calculation is supposed to be 3000°K.

4.2 Sensitivity studies to model parameters

In this chapter, some sensitivity results to model parameters variations are presented which show their influence on the overall flame structure: Some of these parameters can be directly linked to the calculation domain definition (mesh grid), others depend on the aluminized propellant composition (gases flow rate, Al droplets injection rate) or directly define the droplets thermal behavior (droplets initial temperature).

In these simulations, the Al droplets injection rate appears to drive at the first order the overall structure of the flame.

Sensitivity to model parameters

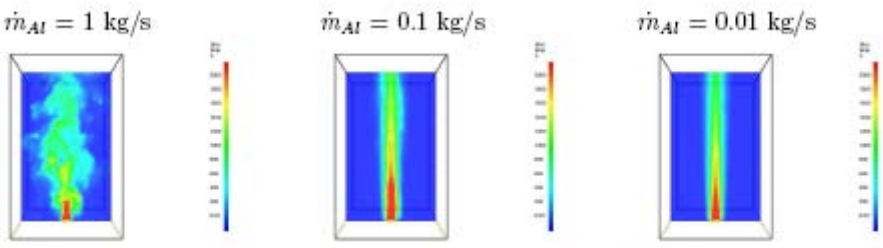

Figure n° 15: Influence of Al droplets injection rate on flame structure

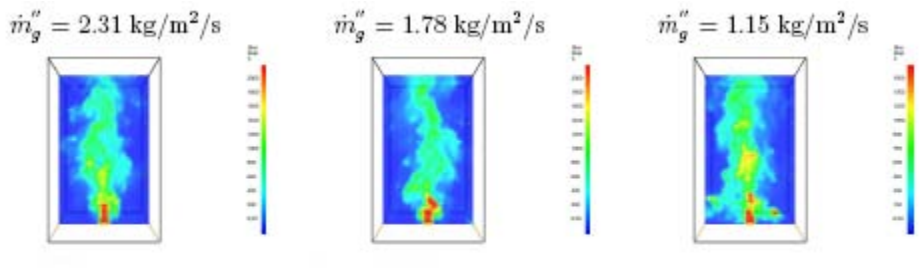

Figure n° 16: Influence of gas flow rate on flame structure

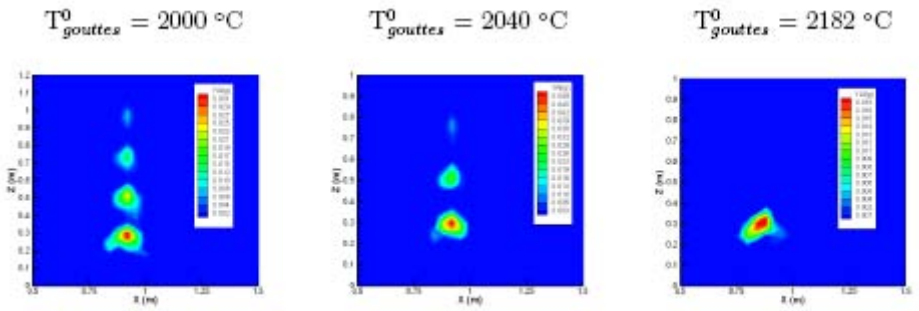

Figure n° 17: Influence of initial droplets temperature on vaporization

A lot of parameters are introduced in the model to take into account the physics complexity of that type of fire and it penalizes a little the sensitivity studies. More over, each model taken separately is based on assumptions valid on limited cases: for instance, the droplet combustion model suppose a laminar gaseous flame regime and introduce a mixture fraction as a new parameter which requires very fine meshes to allow Al gas and oxygen reaction.

4.3 Comparison with experiments: large view tests

The domain is a 5m * 5m * 3m volume with a uniform and structured mesh of 125 * 125 * 100. This means typically 200 h for 10 s simulation on a average personal computer (ref 2008)

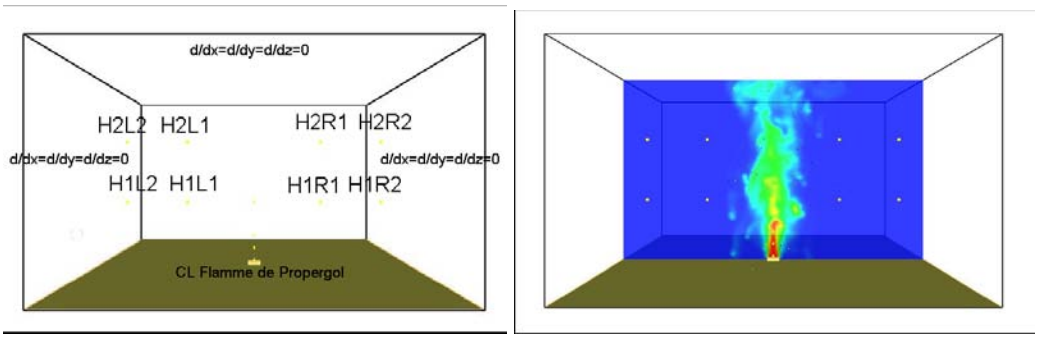

Figure n° 18: Large view test configuration (modeled)

The sensitivity study highlights the Al droplet injection rate as the most influential parameter on the overall flame structure and heat transfer associated with.
For the calculated injection rate, the heat release coming from the Al droplets combustion appears to be too weak compared to experimental results. Due to the low mesh resolution compared to the droplet radius, the Al gas produced by the droplet vaporization does not react sufficiently with the oxygen which is not satisfying.

For higher injection rate up to 1 kg/s, some agreement between experimental results can be found especially for temperatures within the flame with however a generally overestimate of radiative heat fluxes.

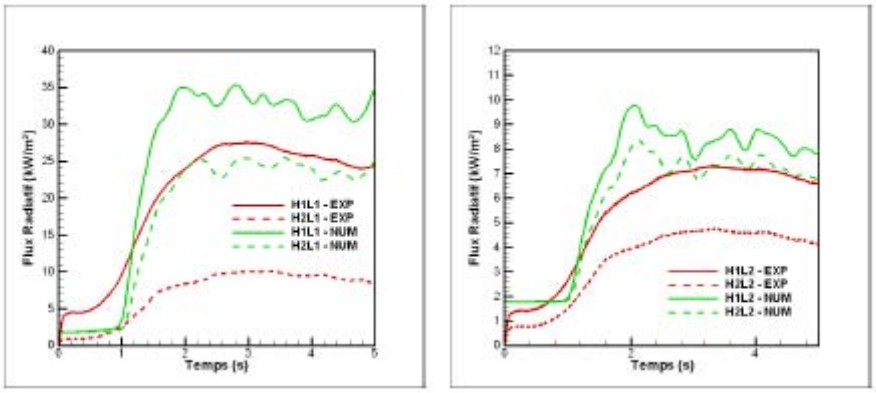

Figure n° 19: Heat flux comparison / outside the flame

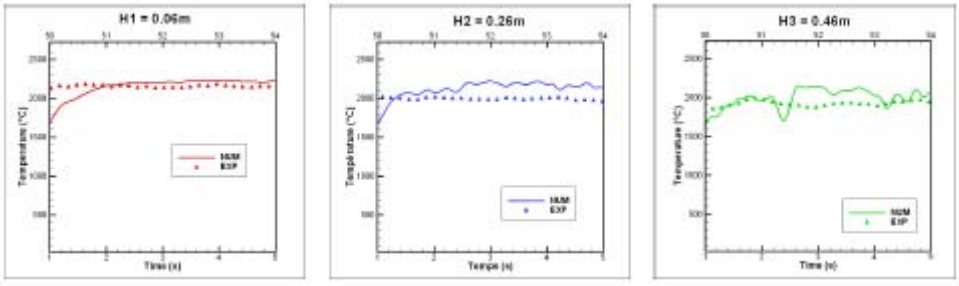

Figure n° 20: Flame temperature vs height

Several axes can be considered for modeling improvement: First of all, it seems important to calculate more precisely the radiative part coming from gaseous species like CO, CO2 and HCl especially for AP/HTPB propellant with low content of aluminum. Then, if the droplet combustion is currently calculated from a mixture fraction model, it appears to be too dependant of mesh size. An option should be to introduce a combustion law function of the droplet diameter (ex. d^2 law) or to couple directly combustion and turbulence.

5. Conclusion

The ultimate goal of this study which started in 2004 is to better address some specific explosive safety issues related to large ambient HTPB/AP aluminized propellant fire and to overcome inherent limitations to current methods based on simple analytical formula and zone models.
More precisely the initial hope was to take fully advantage of all the recent major advances in the field of civilian fire safety engineering by introducing computational fluid dynamics and LES techniques for the part of the physics common to traditional “fuel” fire.
The first difficulty has come from the relative paucity of experimental data in open literature so it has been decided to conduct different scale experiments starting with 20 cm propellant cubical samples to full combustion of LSRM loaded with 2 tons of propellant. Unfortunately, the amount of physical parameters required and not accessible by current instrumentation techniques is a concern and a lot of assumptions were made in the modeling scheme to overcome this lack of knowledge.
The overall trends in terms of flame structure and heat release can be reproduced by modeling but the better results were obtained by “betraying “the representativiy of some physical parameters like the Al droplet distribution in the flow. This is a clear limit of this type of approach and although some improvement axes are considered for further development, the ability of field models to fulfill all the requirements in terms of validation has still to be demonstrated.

Reference

[1] Lengellé, G., Duterque, J. and Trubert, J.F. (2000) *Physico-Chemical Mechanism of Solid Propellant Combustion.* Progress in Astronautics and Aeronautics "Solid Propellant Chemistry, Combustion and Motor Interior Ballistics, Ed. AIAA, NY, pp.287-323.

[2] Beckstead, M.W. (1993) *Solid propellant combustion mechanisms and flame structure.* Pure and Applied Chemistry, 65.2, pp.297-307.

[3] Price, E.W. (1979) *The fire environment of a solid rocket propellant burning in air.* Air Force Weapons Laboratory.

[4] Karasev, V.V., Onishuk, A.A., Glotov, O.G., Baklanov, A.M., Maryasov, A.G., Zarko, V.E., Panfilov, V.N., Levykin, A.I. and Sabelfeld, K.K. (2004) *Formation of charged aggregates of Al2O3 nanoparticles by combustion of aluminum droplets in air.* Combustion and Flame, 138, pp.40-54.

[5] NIST. (2004) *Fire Dynamics Simulation V4, Technical Reference Guide.* NIST Ed.K.McGrattan

[6] Duterque J. and Hommel J. (1993) *Etude de l'agglomération et de la combustion des particules d'Aluminium dans les propergols solides.* La Recherche Aérospatiale, N°4, pp.1-24.

[7] Smagorinsky, J. (1963) *General Circulation experiments with the primitive equations.* Monthly weather review, pp.99-164.

[8] Raithby, G.D. and Chui, E.H. (1990) *A Finite-Volume Method for prediciting radiant heat transfer in encolsures with participating media.* Journal of Heat Transfer, 112(2), pp.415-423.

[9] Diaz, J.C. (1993) *Thermal environment of a solid rocket propellant fire in ambient atmospheric conditions.* JANNAF Combustion Subcommittee Meeting, Ed. Lawrence Livermore Laboratory.

[10] Dombrovsky L. *Possibility of determining the dispersed composition of a two-phase flow from small-angle light scattering. High Temperature* (Teplofiz.Vys.Temp.)

[11] Dombrovsky L. and Ivenskih. *Radiation from a homogeneous plane-parallel layer of spherical particles*. Teplofiz.Vys.Temp., 4 :818. 138

[12] F. Millot V. Sarou-Kanian, J.C. Rifflet. *IR radiative properties of solid and liquid alumina : Effects of temperature and gaseous environment*. International Journal of Thermophysics, 26(4) :1263–1275, 2005.

[13] Duterque J. Hilbert R. and Lengellé G. *Agglomeration et combustion de l'aluminium dans les propergols solides.* Technical report, 1999. 50, 52, 60

[14] Parr T.P. and Hanson-Parr D.M. *AP/htpb/al propellant flame structure at 1 atm.* Technical report, 2006. 50, 60, 61, 166, 171

Liberté • Égalité • Fraternité
RÉPUBLIQUE FRANÇAISE

MINISTÈRE DE LA DÉFENSE

Large solid rocket motor safety analyses: Thermal effects issues

Serge Bordachar – MoD/DGA - IPE
Dr Fabien Chassagne – MoD/DGA - CAEPE

Inspection des Poudres et Explosifs
5bis avenue de la porte de Sèvres
75509 Paris cedex 15

Direction Technique
CAEPE - Avenue Gay Lussac
33167 Saint Médard en Jalles cedex
DGA

Background : Explosive risk management

- **Three general principles :**
  - Source risk reduction
  - Mishap effects limitation (action on propagation vector)
  - Mishap consequences limitation (action on ES)

- **Two regulations coexisting**
  - Health and Safety at Work
  - Environment

Fire phenomenon assessed through modeling

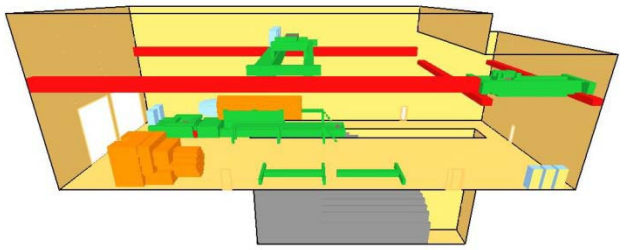

LSRM safety issues

- Managing risk associated with several tons of propellant on the whole life cycle
- Focus on HTPB/AP composite propellants mostly used for large scale applications in France
- The Explosive and Nuclear safety authorities expressed concerns in 2004 regarding :
  - Lack of knowledge on ambient propellant fire phenomenology
  - Use of too conservative methodologies leading to over costs in buildings design and operational difficulties
  - Disparity with civilian methodologies and the “boom” of fire safety engineering

Ambient propellant fire DGA program [2005 – 2011]

- DGA/DT/CAEPE (F.Chassagne)– SME (SNPE group) partnership
- CNRS/Combustion and detonics laboratory

Main goal : Improve propellant fire modeling capability in explosive site studies

Program architecture

MEANS

① Numerical Modeling

Strategy : benefits from CFD and LES techniques in traditional “fuel” fire modeling

(FDS from NIST/BFRL, coupling with propellant combustion code,…)

② Experimental Tests

Refining the existing data, Heat flux measurements, flame temperature in situ measurement with pyrometers and spectrometry, various tests scales

FINAL OBJECTIVE

Assess fire field models maturity and ability to fulfill MoD requirements

Some MoD requirements

Criteria	*Requirement*	*Flexibility*
Specification on input data	Experimental tests on SME HTPB/AP propellant s are to be privileged Literature results are to be used cautiously	Negotiable
Specification on hydrodynamic model	Navier Stockes equations and solid conduction equations must be solved in conditions representative of a fire: this part defines the director schemes to properly simulate a fire and gives some details on the way input data, combustion model, particulates radiative and turbulence models, numerical methods, output data, validation criteria should be presented.	No negotiable Turbulence resolution method to be chosen by university.
Specification on combustion model	A pyrolysis model and a heat generation source term shall be introduced in the model	No negotiable
Specification on radiative heat transfer model	The model must take into account all the radiative exchanges : particles (alumina, Al,…) and gaseous combustion products .If a T4 formulation is used, the model must discriminate between radiative heating inside the flame and outside the flame. A local formulation inside the flame and based on calorific debit ratio is possible	No negotiable Negotiable
Specification on combustion products and particulates	The transport equation can be solved using a species generation term proportional to the combustion rate. Each specie to have its own transport equation.	Negotiable
Specification on boundary conditions	The boundaries conditions must be versatile	No negotiable
Specification on output data	The output data must incorporate both global and local thermal fluxes characteristics , temperature, hydrodynamic data All the information on the present species in the gaseous mesh is to be available	No negotiable
Validation criteria on output results	Validation criteria must be defined	No negotiable
Specification on reports	The reports must enable validation, alter expertise and new simulation studies	Negotiable
Software specification	Open source, Fire Dynamic Simulator from BFRL/NIST privileged	Negotiable

Experimental Tests (1) : Objective

Experimental Tests

Input Data

Flame emissivity

Solid propellant Fire Model

PROPELLANT FIRE MODEL VALIDATION

Results Comparison

Radiative Heat Flux, burning rate, temperature, …

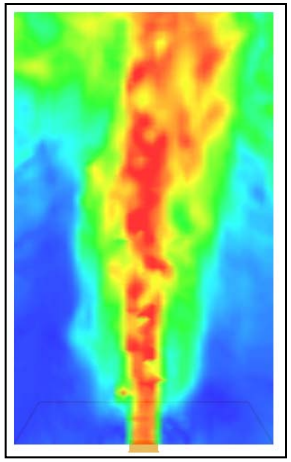

Experimental Tests (2) : Large View Tests

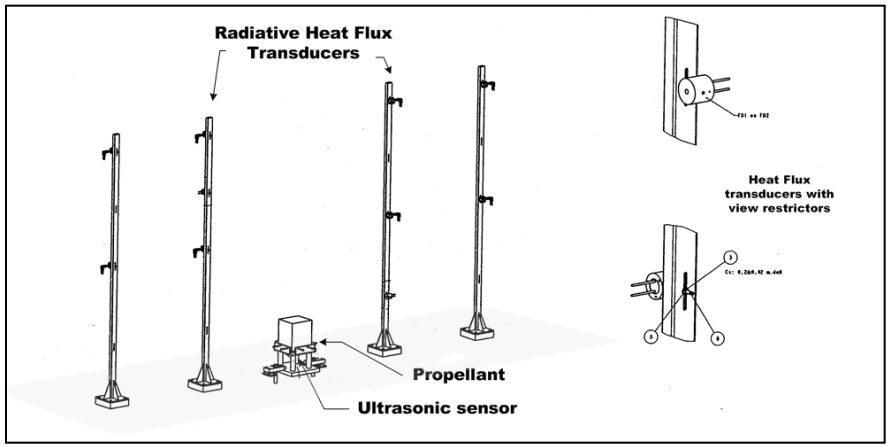

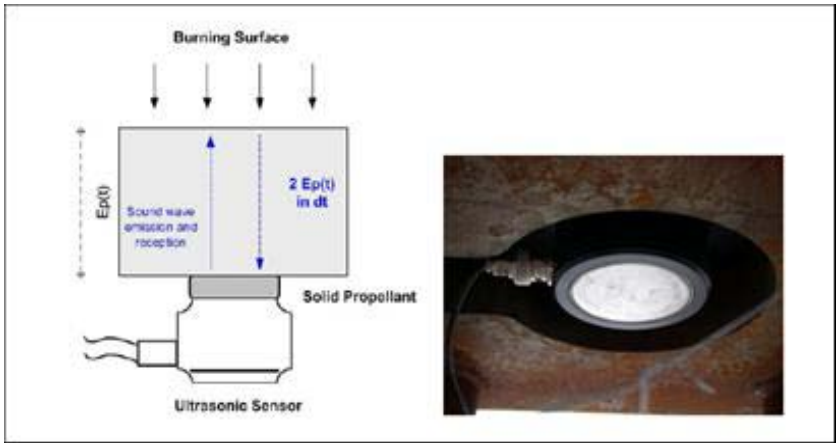

- Radiative Heat Flux Measurements
- Burning rate measurements by Ultrasonic system
- IR and UV flame plume signature

Experimental Tests (2) : Tests within chimney

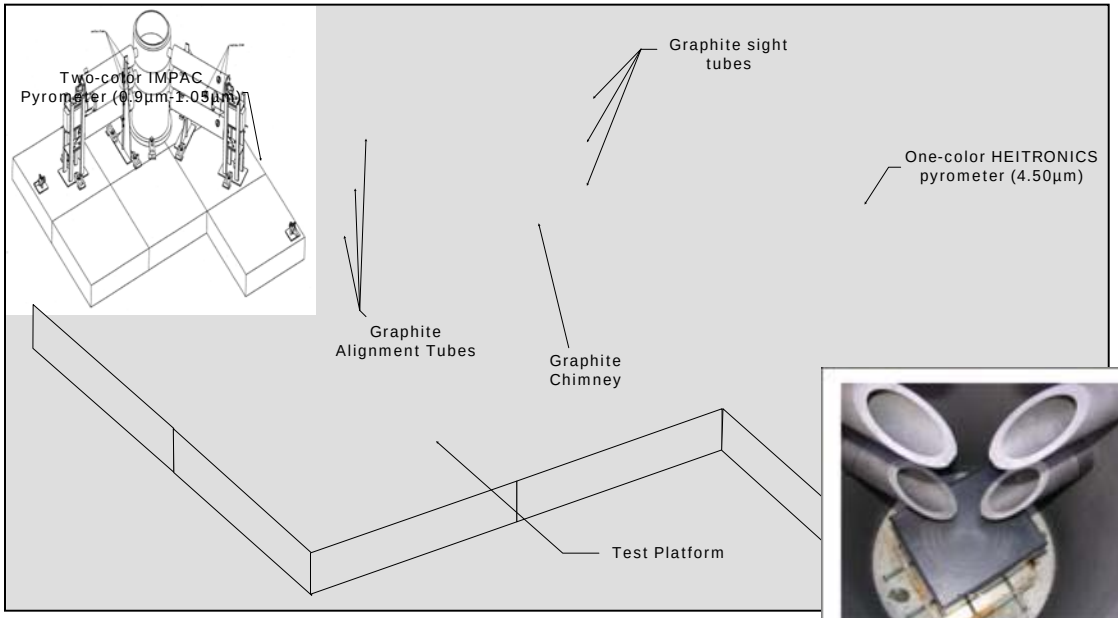

- Local flame temperature by two-color pyrometers
- Local monochromatic emissive flame properties by one color vs. two-color pyrometer association

Large scale experimental Tests (3)

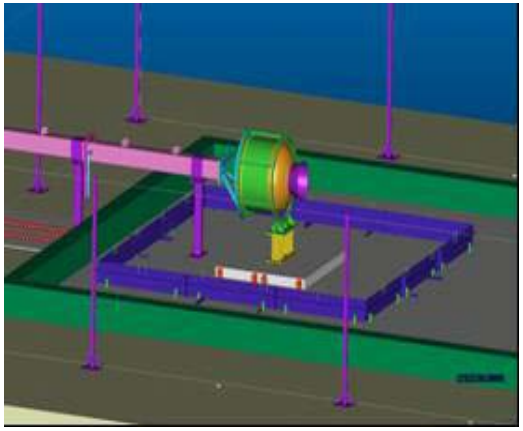

Fuel fire on a LSRM (third stage M45 missile, 2 tons of propellant) – June 2010 - classified

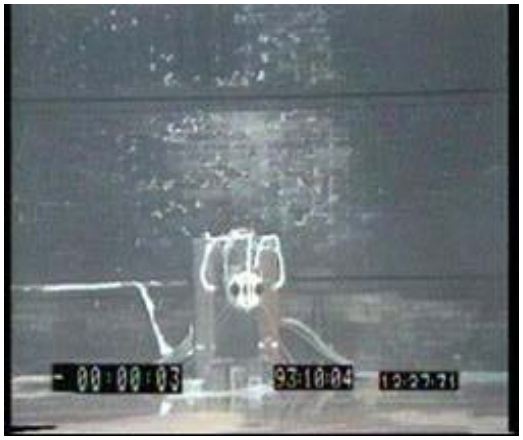

1 m² surface propellant fire on hardware internally instrumented with thermocouples for reverse engineering

Numerical Modeling (1)

- Based on FDS.v4 code (Fire Dynamics Simulator)
  - Low Mach number assumption
  - 3D Large Eddy Simulation
- Modifications of the original source code (Fortran 90)

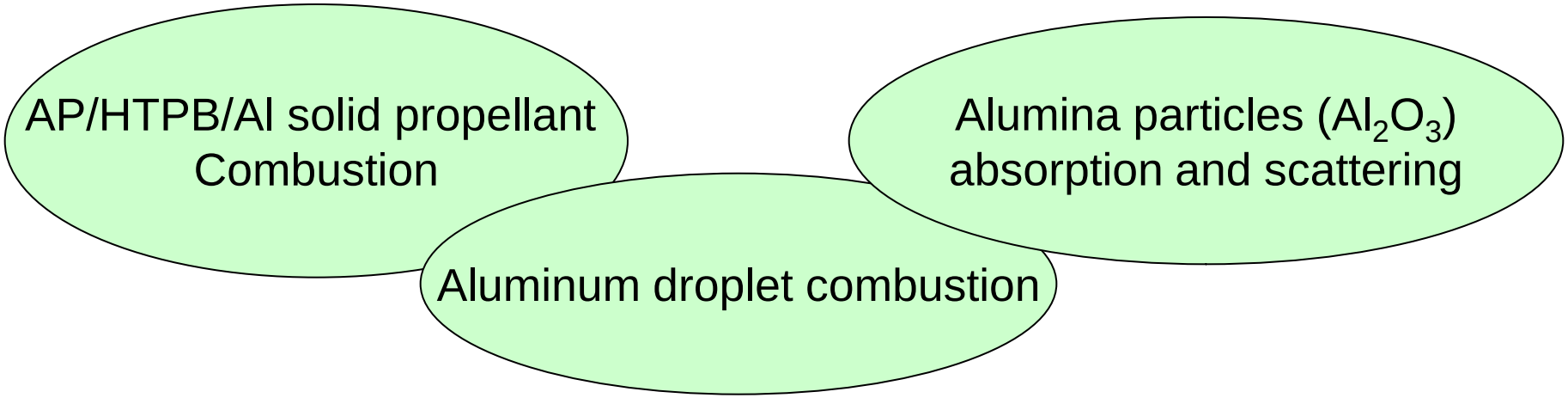

AP/HTPB/Al solid propellant fire model

Sensitivity studies (ex.)

- Influence of Al droplets injection rate on flame structure

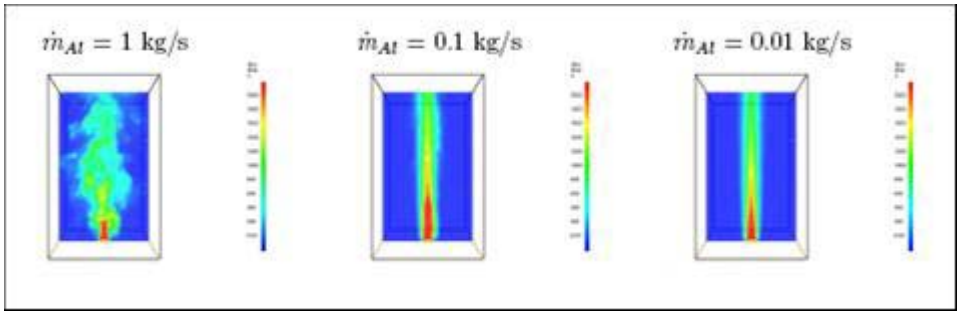

- Influence of gas flow rate on flame structure

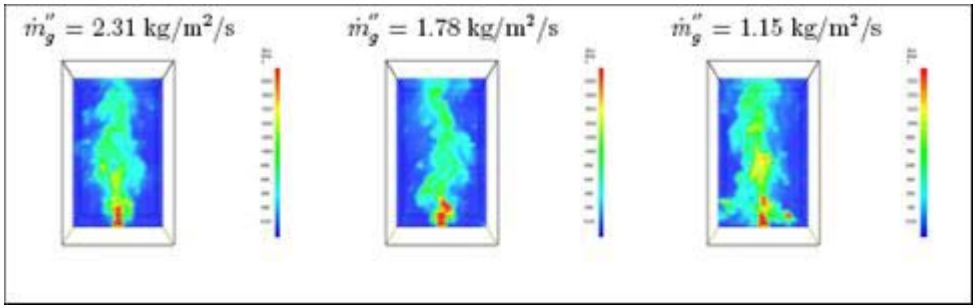

Sensitivity studies (ex.)

- Influence of initial droplets temperature on vaporization

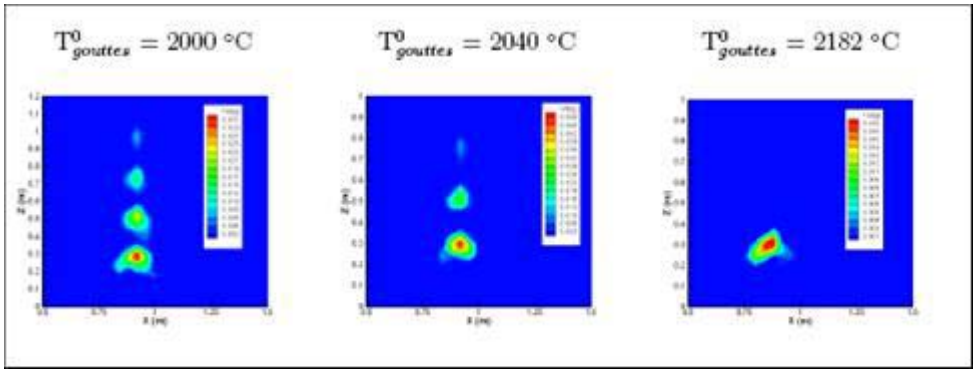

Conclusion on sensitivity studies :

Al droplets injection rate is the most influential parameter driving the overall flame structure with our hypothesis.

Large view test modeling

- Modeling vs. large view tests results

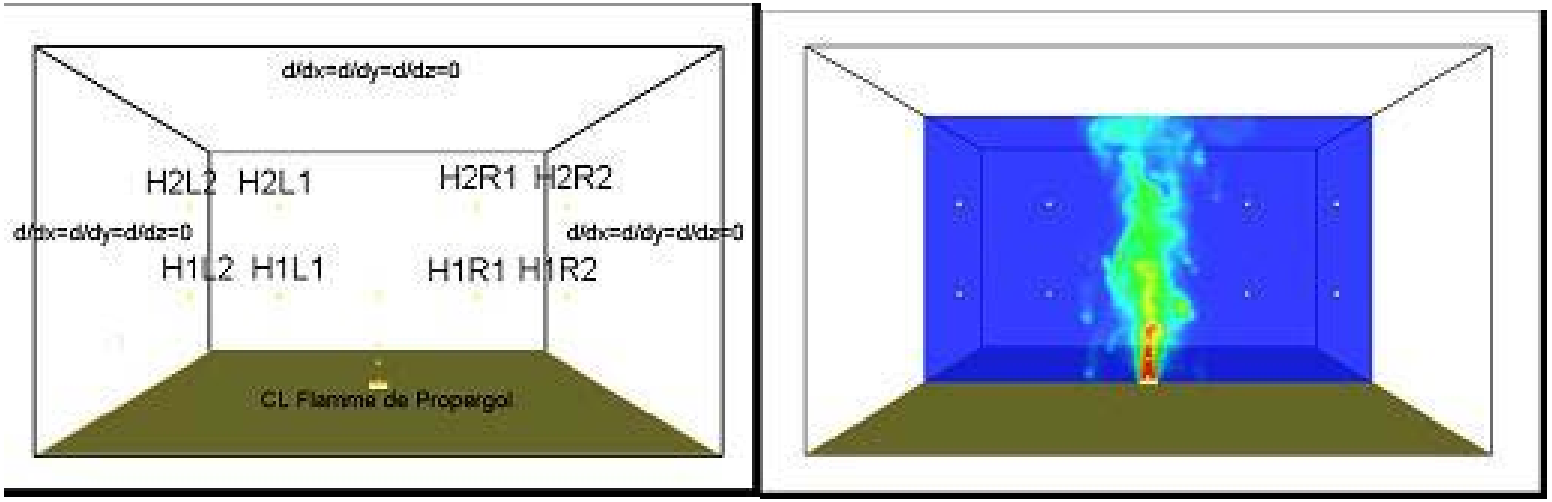

The domain is a 5m * 5m * 3m volume with a uniform and structured mesh of 125 * 125 * 100. This means typically 200 h for 10 s simulation on a average personal computer

Large view test modeling (2)

- Heat flux comparison / outside the flame

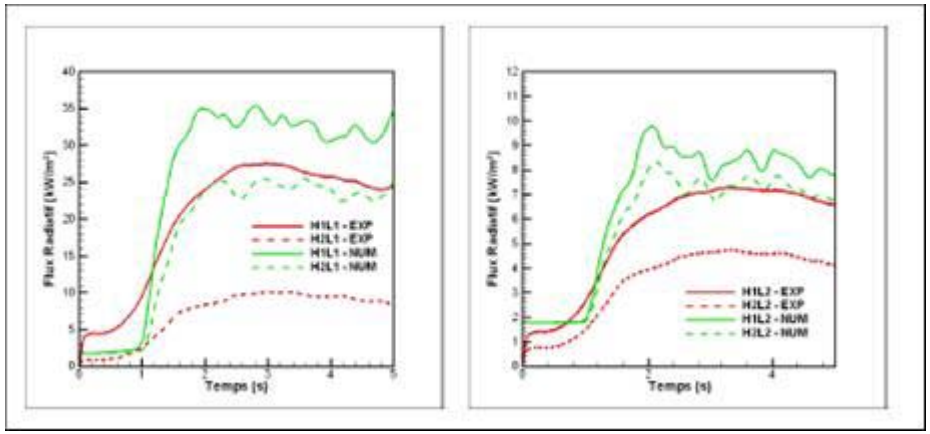

- Flame temperature

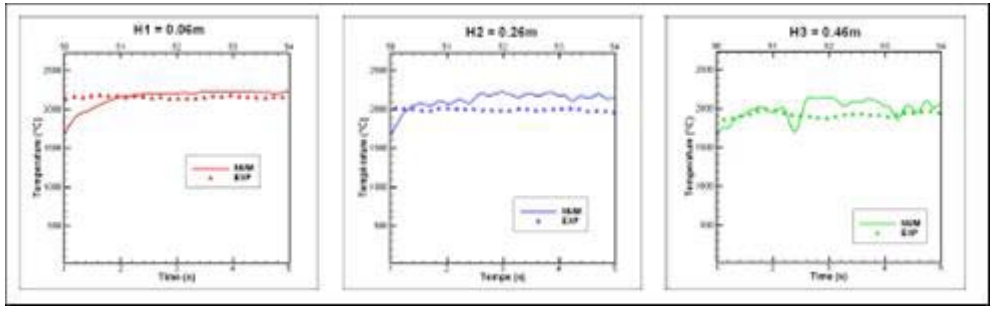

Comments on modeling results

- For the calculated injection rate, the heat release coming from the Al droplets combustion appears to be too weak compared to experimental results. Due to the low mesh resolution compared to the droplet radius, the Al gas produced by the droplet vaporization does not react sufficiently with the oxygen which is not satisfying.
- For higher injection rate up to 1 kg/s, some agreement between experimental results can be found especially for temperatures within the flame with however a generally overestimate of radiative heat fluxes.
- The droplet combustion currently calculated from a mixture fraction model is too dependant of mesh size. An option should be to introduce a combustion law function of the droplet diameter or to couple directly combustion and turbulence.

Conclusion

- The amount of physical parameters required and not accessible by current instrumentation techniques is a concern and a lot of assumptions were made in the modeling scheme to overcome this lack of knowledge .

- The overall trends in terms of flame structure and heat release can be reproduced by modeling but the better results were obtained by “betraying “the representativity of some physical parameters like the Al droplet distribution in the flow.

- Some results especially regarding the experimental side are promising but the ability of field models to fulfill all the MoD requirements in terms of validation has still to be demonstrated